Cell Tissue Res (2007) 329:221–230
DOI 10.1007/s00441-007-0413-7

REGULAR ARTICLE

Vagal innervation of intestines: afferent pathways mapped with new en bloc horseradish peroxidase adaptation

Feng-Bin Wang · Terry L. Powley

Received: 6 February 2007 / Accepted: 6 March 2007 / Published online: 24 April 2007

Abstract Neural tracers have not typically been employed to determine the pathways followed by axons between their perikarya and target tissues. We have adapted the tetramethylbenzidine method for horseradish peroxidase (HRP) to stain fibers *en bloc* in organs and thus to delineate axonal trajectories. We have also applied this protocol to characterize the pathways that vagal afferents follow to the intestines. The protocol confirms that the proximal segment of the duodenum receives afferents carried in the vagal hepatic branch and demonstrates that vagal afferents innervating the remainder of the small and large intestines course through multiple fascicles derived from the celiac branches of the abdominal vagus. These fascicles divide, intermingle, and reorganize along the abdominal aorta and superior mesenteric artery (SMA), but not along the inferior mesenteric artery, and then project to the intestines with secondary arteries that branch from the SMA. The inferior pancreaticoduodenal, jejunal, middle colic, right colic, and ileocecocolic arteries all carry vagal afferents to segments of the intestines. As the arteries derived from the SMA divide repeatedly into successively finer branches and course to the intestines, the vagal afferent fascicles (typically a pair) running with each arterial branch also divide. These divisions generate sets/pairs of finer fascicles coursing with even the highest order arterial radicles. The vagal fascicles enter the intestinal wall with the vessels and appear to innervate the organ near the point of entry. The results verify the practicality and sensitivity of the *en bloc* HRP technique and suggest that the protocol could delineate other peripheral pathways.

Keywords Autonomic · Neural tracers · Mesentery · Parasympathetic · Visceral afferents · Rat (Sprague Dawley, male)

This work was supported by grants from the Fulbright-Hays (Fulbright scholarship) and NSC 42114F Exchange Programs and by NSC86-2418-H-194-003-T to F.B.W., and by the National Institute of Diabetes and Digestive and Kidney Diseases, NIH (DK27627 and DK61317) to T.L.P.
The present observations were reported in part at the 2005 annual meeting of the Society for Neuroscience.

F.-B. Wang (✉)
Department of Psychology, National Chung Cheng University, Chia-Yi 62102, Taiwan
e-mail: psyfbw@ccu.edu.tw

T. L. Powley
Department of Psychological Sciences, Purdue University, West Lafayette IN 47907, USA

Introduction

Neural tracers have substantially refined the descriptions of peripheral nerve circuitry. For example, the vagal projections to the intestines have been analyzed previously with conventional tracer methods. Here, however, these pathways have been re-examined with a novel *en bloc* horseradish peroxidase (HRP) processing protocol.

Retrograde experiments have established that the somata of the vagal efferent neurons projecting to the intestines are located in the dorsal motor nucleus of the vagus (Altschuler et al. 1993; Hopkins et al. 1996; Zhang et al. 1991). Specifically, these preganglionic neurons innervating the intestines are located predominantly in the lateral columns within the dorsal motor nucleus and project through the celiac branches (Fox and Powley 1985; Powley et al. 1987), although some of the preganglionic somata are located in the more medial gastric and hepatic columns of the dorsal motor nucleus and project through the gastric and hepatic branches of the subdiaphragmatic vagus, respectively

(Altschuler et al. 1991; Zhang et al. 1991, 2000). Retrograde labeling experiments have also indicated, based on the intestinal loci at which tracer injections produce effective labeling of efferent and afferent neuronal somata, that both vagal preganglionic neurons and nodose ganglion visceral afferents innervate the intestines over virtually their entire length (Altschuler et al. 1991, 1993; Zhang et al. 1991, 2000).

Anterograde experiments involving the application of tracers to dorsal motor nucleus neurons have labeled vagal efferent terminals in the gastrointestinal (GI) tract and made it practical to characterize their distributions and morphology (e.g., Holst et al. 1997). In addition, orthograde tracer observations have established that the vagal afferents with somata in the nodose ganglion innervate intestinal smooth muscle (submucosa and mucosa). Anterograde tracer protocols have also been used to describe the specialized terminal endings and regional patterns of the various projections (Berthoud and Powley 1992; Berthoud et al. 1995; Phillips et al. 1997; Powley and Phillips 2005; Wang and Powley 2000). Most notably in terms of the present report, anterograde tracing has shown that vagal afferents supply terminal endings to the intestines, from the duodenum to the colon (Wang and Powley 2000).

For some applications, such tracer observations concerning the origins or the distributions of terminals within target tissues are the only kinds of information needed. In other situations, however, information about the precise trajectories that particular projections follow is required. Exact details of the pathways that axons travel between their origin and their termini become critical if, for example, a specific nerve bundle has to be isolated for recording, highly selective denervations have to be generated, or a pathway must not be inadvertantly compromised during an invasive procedure.

In previous wheat-germ-agglutinin/horseradish-peroxidase (WGA-HRP) studies of vagal projections, we have been impressed by several features of the tracer protocol that suggest the technique can be adapted so as to trace axons along their full trajectories. (1) In relatively thick sections or flat whole-mounts of GI smooth muscle, WGA-HRP processing can effectively reveal not only axonal trajectories within the organ wall, but also terminal fields (Powley and Phillips 2005; Wang and Powley 2000). (2) The solutions employed in WGA-HRP processing have few problems penetrating tissue, suggesting that the tracer might be used with organ preparations that are even more extensive than GI tract whole-mounts. (3) WGA-HRP is taken up by virtually all vagal axons (Phillips et al. 1997; Robertson et al. 1992; Wang and Powley 2000), making the marker useful for a comprehensive inventory of the projections. (4) WGA-HRP is transported effectively in both retrograde and anterograde directions (e.g., Mesulam 1982; Powley and Phillips 2005), so that when it is injected near either peripheral or central neurites of afferent neurons, it is incorporated, carried to the somata, and then also distributed transganglionically into the opposite neurite.

In the series of experiments described here, we have adjusted the fixation and processing steps of the tetramethylbenzidine (TMB) technique (Mesulam 1978, 1982) successfully to process large tissue specimens (whole GI organs or viscera), so that the WGA-HRP labeled vagal fibers are preserved *in situ*. Such specimens make it practical to establish the paths or trajectories of the distal branches of the nerve as they course to their targets. This report both illustrates the *en bloc* technique and characterizes the pathways by which vagal afferent fibers reach the small and large intestines.

Materials and methods

Male Sprague-Dawley rats (175–250 g) were anesthetized with Nembutal (60 mg/kg, i.p.). In some animals, either the left (n=14) or right (n=14) nodose ganglion or the dorsal medulla (n=32) was exposed; in other animals (n=3), both nodose ganglia were exposed. Each animal received a pressure injection (Picospritzer II, 11.25 kg pressure; 3–6 ms/pulse) of WGA-HRP (4% solution in a salt buffer supplied by Vector Laboratories, Burlingame, Calif.; Cat. No. PL-1026) into the left, right, or both nodose ganglia (0.5–1.0 μl total volume per side) or the nucleus of the solitary tract (three injection sites per side; 0.5–1.0 μl total volume). At the time of the injections, some animals were also given unilateral cervical vagotomies (n=3) or ventral root motor rhizotomies (n=10) ipsilateral to the nodose ganglion tracer injections, according to the technique of Walls et al. (1995). One group (n=20) of the injected animals was assigned to analyses of the "descending aorta to superior mesenteric artery (SMA) to intestinal pathways'; a second group (n=15) of animals was used to evaluate whether vagal afferents innervating the intestines traveled from the descending aorta to the inferior mesenteric artery to reach the intestines.

On day 2 or 3 after tracer injection (time depending on transport distance involved), each rat received an overdose of Nembutal (180 mg/kg, i.p.) and was then perfused transcardially with warm saline (250 ml, 37°C) followed by 3% paraformaldehyde and 0.2–0.4% glutaraldehyde in 0.1 M phosphate buffer (250 ml, 4°C, pH 7.3–7.5), and 10% sucrose in phosphate buffer (150 ml, 4°C, pH 7.3–7.5).

All protocols were conducted in accordance with the Principles of Laboratory Animal Care (NIH publication no. 86-23, revised 1985) and the guidelines of the American Association for Accreditation of Laboratory Animal Care.

Approval for all these protocols was also obtained from the Purdue University Animal Care and Use Committee.

Tissue specimens including appropriate organs were then taken *en bloc*. Specimens for examination of the vagal trunks and primary branches consisted of the subdiaphragmatic esophagus, the stomach with associated vessels and attachments, and the proximal-most segment of the duodenum (bulb). Blocks for examination of the distal vagal branches innervating the intestines consisted of a segment of descending aorta and the appropriate vessels and mesentery. In most cases, the block of vessels and mesentery was trimmed from the duodenum, jejunum, ileum and colon just at the intestinal mesenteric attachment. If necessary, the vessels and hollow organs were flushed or cleared of contents with saline or water. For improvement of exposure, some abdominal fat was removed from the specimens by dissection. Similarly, in order to eliminate tissues that contained excess secondary or non-specific reaction product (e.g., mast cell staining) that would otherwise obscure specific labeling, tissues were dissected or teased apart. In some cases, for example, the mucosa and submucosa were peeled from intestinal smooth muscle whole-mounts either before or after the HRP-TMB reaction.

In general, the blocks of abdominal tissues were processed according to the TMB protocol of Mesulam (1978, 1982). Fixative concentrations, however, were reduced (see above). Furthermore, for post-perfusion storage, a 10% solution of sucrose in phosphate-buffered saline (no fixative) was used, and the storage time was minimized. After any trimming or removal of adipose tissue, the tissues were rinsed twice with distilled water before the HRP-TMB reaction was performed. To achieve the appropriate degree of labeling, the reaction was typically run in as a series of successive steps (~3–5 min) separated by inspections of the tissue with a surgical microscope.

After the HRP-TMB reaction, specimens were arranged on uncoated slides or Parafilm for purposes of low-power macrophotography. Once macrophotographs had been taken, excess and extraneous tissue was removed from the block (to minimize specimen thickness), and the labeled tissue was then transferred to a gelatin-coated slide. For purposes of coverslipping, the specimens were covered with non-stick-coated (Sigmacote, Sigma) glass slides and flattened with weights for 30 min. The top (non-sticking) slides were removed, and the specimens were then air-dried at room temperature overnight and cleared twice with xylene (5 min each); after prior air-drying, ethanol proved unnecessary for the dehydration and was not used because it tended to fade the TMB chromogen. Because of the tissue thickness and the numerous vessels and ducts, there was a tendency for the specimen to trap air. To minimize this problem, air bubbles within the vessels were excluded by pressing the tissue with a spatula while it was immersed in xylene. Specimens were coverslipped with DPX neutral mounting medium (Aldrich, Milwaukee, Wis.).

Low-power images of the labeled specimens were obtained with a digital camera (Nikon CoolPix 995 or 8400). Higher power images were taken with a Spot RT Slider cooled charge-coupled device digital camera (Diagnostics Instruments, Sterling Heights, Mich.) on a Leica DMRE microscope. Photoshop CS software (Adobe Systems, Mountain View, Calif.) was used to (1) adjust brightness, contrast, and color balance; (2) apply scale bars and text; (3) organize the final layouts of the plates.

Results

Validating the *en bloc* procedure

The *en bloc* protocol produced excellent staining by WGA-HRP within the vagal afferents, without any sectioning or extensive dissection of the tissues. As a means of initially validating the protocol before examination of the projections to the intestines, the pattern of staining of the abdominal vagal trunks and their primary branches and the staining of the vagal innervation within the stomach wall achieved with the *en bloc* protocol were examined and compared with established descriptions of the subdiaphragmatic vagus (e.g., Boekellar et al. 1987; Powley et al. 1983; Prechtl and Powley 1985, 1990).

These patterns are illustrated (Fig. 1a) in an animal in which the peripheral vagal afferents had been labeled transganglionically by WGA-HRP injections into the nucleus of the solitary tract bilaterally. Figure 1a also shows the ventral or anterior surface of the abdominal esophagus, stomach, and duodenal bulb. In the conventional pattern, the ventral trunk of the vagus travels down the esophagus and gives off a (hepatic) branch that leaves the esophagus in conjunction with a (hepato-esophageal) vessel. The heaviest vagal bundle, the ventral gastric branch, continues along the esophagus, giving off another branch (the accessory celiac) that wraps around and disappears behind the esophagus. The gastric branch then continues onward, dividing into secondary branches that fan out over the stomach.

The view of the ventral stomach wall from the surface (serosa still covering the organ) illustrates that the *en bloc* processing protocol is able to penetrate into the organ to label the myenteric plexus. In this example, the labeled vagal afferent axons effectively define the network of connectives of the plexus, and the labeled terminals in the ganglia (intraganglionic laminar endings) delineate the individual ganglia of the myenteric plexus.

Validation by using the intact blocks of esophagus, stomach, and duodenal bulb verified that the protocol was able to detect the details of vagal architecture in the

abdomen, even including such features as the occasionally observed doubling of the ventral trunk on the more rostral esophagus (cf. Fig. 1a). Furthermore, another validation step by using cervical vagotomy contralateral to a brainstem injection and ventral vagal rhizotomy ipsilateral to the injection established which cervical vagal trunk carried the labeled axons and that the label was afferent (i.e., unaffected by ventral root rhizotomy).

Experiments with the stomach block also verified that, by varying the length of time that the reaction was allowed to run, even the finer fascicles could be stained, and the specimens could be readily penetrated allowing labeling of the deeper innervation elements. In Fig. 1b, for example, the definition of the myenteric plexus in the wall of the stomach is still light, whereas in Fig. 1a, the plexus is accentuated after lengthening of the incubation interval.

Fixative concentration and length of exposure were also critical in determining the completeness of staining. Lower concentrations of paraformaldehyde and glutaraldehyde left the tissue poorly fixed, and the TMB labeling tended to fade relatively rapidly. Higher concentrations of paraformaldehyde and/or glutaraldehyde (particularly glutaraldehyde) reduced penetration and TMB staining. In our experience, the fixative concentrations given in Materials and methods (lower than those typically used for HRP processing) provided the best compromise between inadequate and excessive fixation.

Vagal afferent pathways to intestines

Consistent with other anatomical observations (e.g., Prechtl and Powley 1987; Phillips et al. 1997; Wang and Powley 2000), the hepatic branch of the subdiaphragmatic vagus bifurcated after separating from the esophagus. One of the secondary branches provided innervation to the initial segment or bulb of the duodenum, and labeled afferent fibers were consistently seen branching to the proximal duodenal wall (Fig. 1b). Since this pathway is well known (and is currently under examination in detail), most of the present observations focus on the vagal afferents that follow circuitous (and less well established) paths to the more distal intestinal field.

The two vagal branches that carry most of the intestinal vagal projections, namely the celiac branches, can be seen in Fig. 1b; this specimen has been rotated around the long axis of the esophagus so that both the ventral vagal trunk (to the right side of the esophagus) and the dorsal vagal trunk (to the left side) can be seen. The dissected accessory celiac branch is displayed and reflected from the esophagus at the point where it separates from the ventral trunk, wraps counterclockwise, and would normally disappear dorsal to the esophagus. The dissected celiac branch is displayed separating from the dorsal vagal trunk and travels in the direction of the abdominal aorta.

Fig. 1 Specimens of esophagus, stomach and proximal duodenum processed with the *en bloc* protocol. **a** The vagal afferents were labeled by bilateral injections of WGA-HRP into the nucleus of the solitary tract. The ventral or anterior vagal trunk (see *two white arrowheads* at a point before further bifurcation) travels down the esophagus and gives off the hepatic branch (*Hep*), which runs deep into the omentum. The ventral trunk continues distally for a short distance where it again divides into the accessory celiac branch (*ACB*), which wraps counterclockwise to disappear dorsal to the esophagus, and the ventral gastric branch (*VGB*), which continues on toward the stomach, bifurcating again just proximal to the lower esophageal sphincter. Within the ventral wall of the stomach, the labeled vagal fibers delineate both the connectives and ganglia of the myenteric plexus (*DGB* dorsal gastric branch, *DUO* duodenum). **b** A specimen of esophagus and stomach reserved to expose the dorsal vagal trunk (*DVT*) and to illustrate the two celiac branches (*ACB* accessory celiac branch, *CB* celiac branch) that provide vagal innervation to the intestines from the proximal duodenum to the initial part of the descending colon. Vagal afferents are labeled by bilateral injections of WGA-HRP into the nucleus of the solitary tract. The specimen has been rotated on the long axis of the esophagus so that ventral vagal trunk (*VVT*) appears to travel to the *right* of the esophagus, giving off, at its first bifurcation, the hepatic branch (*Hep*) running clockwise into the omentum (where the branch bifurcates into a hepatic proper division and a gastrointestinal division). The ventral trunk then divides again, giving off the accessory celiac branch (*ACB*), which wraps counterclockwise to run dorsally behind the esophagus (the accessory branch has been reflected *right* at the point where it would normally course out of view), and the ventral gastric branch (*VGB*), which continues down the esophagus and divides again just above the region of the lower esophageal sphincter. The dorsal vagal trunk appears on the *left* side of the esophagus. After the trunk courses dorsal to the hepatic branch, it divides into two branches that have been sectioned and reflected for display. The first of the two branches, coursing perpendicular to and away from the esophagus, is the celiac branch (*CB*); the second of the two, coursing parallel to and more distally with the esophagus, is the dorsal gastric branch (*DGB*) of the vagus. The gastric myenteric plexus is lightly delineated (*arrowhead*), particularly *lower left* (*DUO* duodenum). **c** Another *en bloc* processed specimen of the esophagus, stomach, and initial segment of the duodenum. In this specimen from an animal that had received a left nodose ganglion injection and a left motor rhizotomy (validation steps to establish that all labeling was of left nodose afferents), the labeled afferents coursing in the hepatic branch (*Hep*) can be seen separating into fascicles that innervate the stomach (*bottom*) and the duodenum (*DUO*, *upper left*). Fine fascicles of labeled afferents can also be seen running in the body of the esophagus to the *right* of the heavily labeled anterior vagal trunk and in the proximal stomach. *Bars* 1 cm

Figure 1c illustrates another gastric/duodenal specimen from a different perspective and illustrates afferents from the hepatic branch of the vagus traveling first with the common hepatic branch and then arcing distally toward the proximal duodenum with an unstained vessel (the gastroduodenal artery). As this fascicle of afferents derived from the hepatic branch nears the duodenum, it divides into several finer fascicles that run to the initial segment of the duodenum, with another of the fascicles.

In Fig. 2, which contains two views of the same specimen of a SMA and its derivative arteries, additional

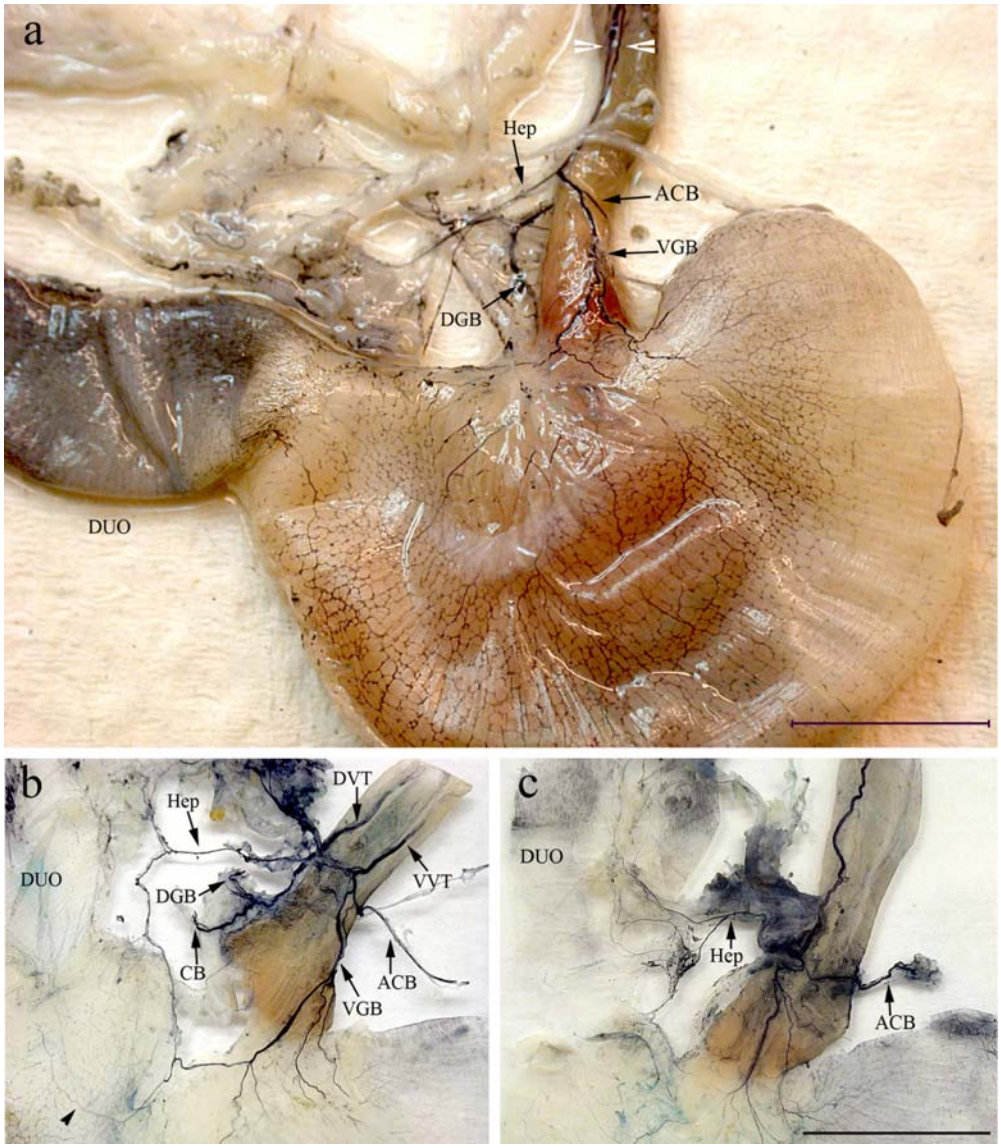

practical features of the *en bloc* HRP method are illustrated. The pattern of the largest contingent of vagal afferents can be seen coursing to the intestines. In Fig. 2a, the specimen is shown in a fresh condition immediately after TMB processing and rinsing; the specimen is still hydrated. In contrast, Fig. 2b displays the same specimen after it has been flattened, dehydrated, and cleared. In Fig. 2b, additional details and the HRP-labeled fascicles are readily observed. As the two views suggest, the *en bloc* TMB processing of the WGA-HRP-labeled bundles of vagal fibers is satisfactory and apparently complete, although the transparency of thick pieces of fresh tissue still containing water limit easy visualization of the labeling.

The *en bloc* method made it practical to follow and characterize the course of the intestinal innervation from the point where the two celiac branches separated from their respective vagal trunks on the esophagus (see Fig. 1a) to the point where their axons entered the wall of the intestine (see Fig. 3c). As reported in dissection studies and in conventional histological descriptions of the paired celiac branches, once these branches separated from the esophagus and traveled dorsally, they coursed parallel to and in association with the left gastric artery, subsequently continuing with the parent the celiac artery, to the abdominal aorta. At the point at which the two primary celiac branches had reached the aorta, they had separated into multiple secondary (or even higher order) bundles (Fig. 2b). These bundles or fascicles then appeared to divide and recombine in loose fasciculated groupings. They then continued on to the intestines and coursed onto the unpaired SMA (Fig. 2b).

As the multiple fascicles from the vagal celiac branches traveled along the SMA (bottom of Fig. 3a), they appeared to re-sort and to recombine. The afferent fascicles then

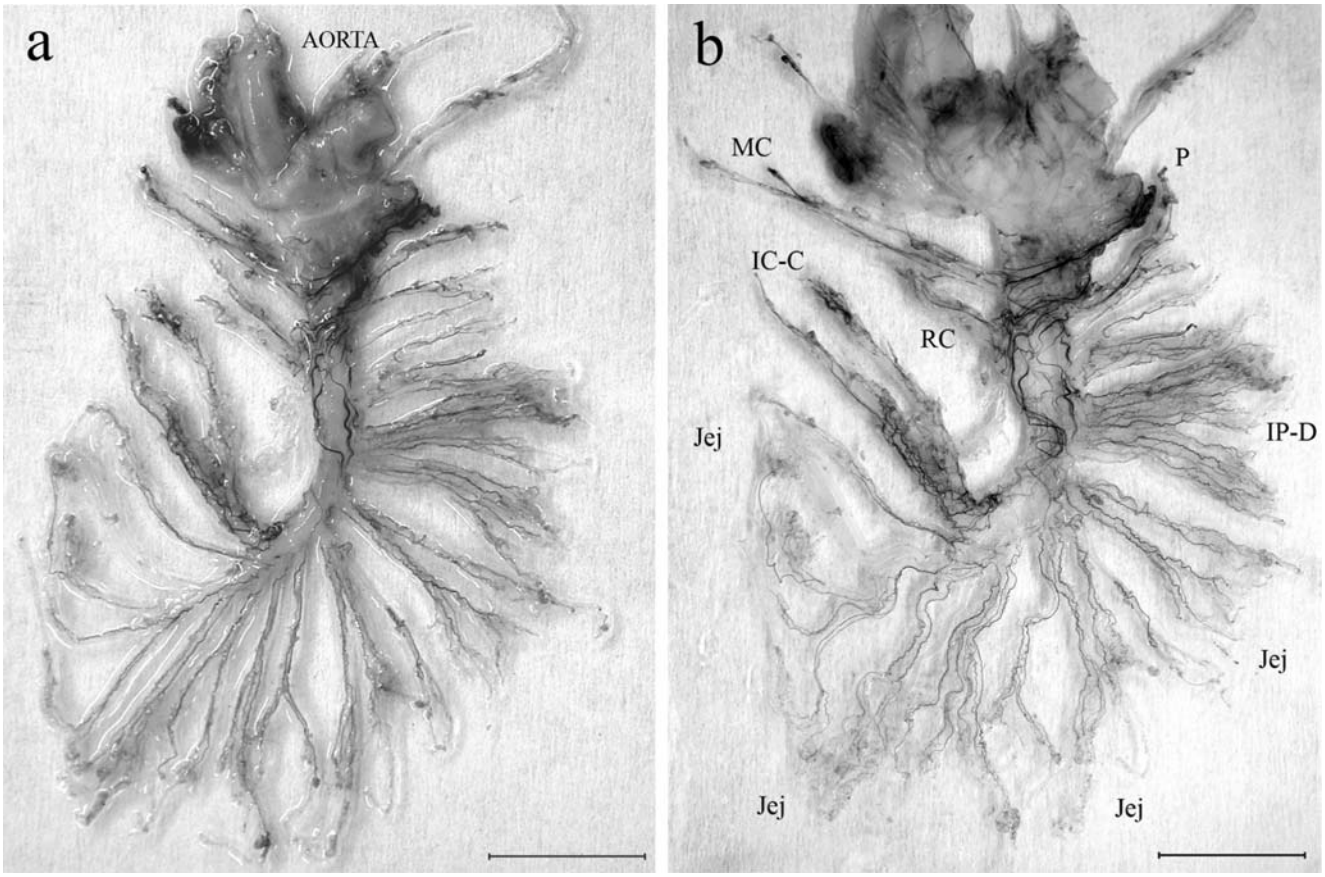

Fig. 2 **a** *En bloc* processed specimen of the descending aorta and superior mesenteric artery (SMA) and its higher order arterial branches taken from an animal that had received bilateral injections of WGA-HRP into the nucleus of the solitary tract. This specimen was photographed immediately after TMB processing, specifically before the tissue was cleared, and while the processed specimen was still hydrated. The plexus of nerve bundles containing labeled vagal afferents can be seen on the SMA descending from the aorta. Bundles of vagal afferents are also present on many of the uncleared arterial branches given off by the unpaired SMA. The SMA and its branches course so as to supply vascular radicles to the intestines, from the duodenum (and pancreas) to the descending colon. **b** The same *en bloc*-processed specimen after it had been dehydrated, cleared with Xylene, and flattened. The paired bundles of vagal afferents on each of the arterial branches are more plainly visible, illustrating that penetration occurs readily in the *en bloc* adaptation of the TMB method. The branches are designated after the nomenclature of Boekellar et al. (1985; see also Hebel and Stromberg 1976). The *en bloc* method reveals the complexity of the fasciculation and branching of the vagal afferents, which obviously distribute with each of the different arteries that derive from the SMA (*IC-C* ileoceco-colic arterial branches, *IP-D* inferior pancreatico-duodenal arterial branches, *Jej* jejunal branches, *MC* middle colic branch, *P* pancreatic arterial branches, *RC* right colic arterial branch). *Bars* 1 cm

passed along successive arterial branches leaving the parent SMA, and labeled axons joined the arterial branches to travel superficially along the arteries. A striking feature of this pattern was that the vagus contributed labeled afferent fibers to virtually all (including both major and minor) arterial branches separating from the SMA (Fig. 2b). Approximately 20 arterial branches separated from the parent SMA. These arterial branches each bifurcated into finer branches three or four times before reaching the intestinal wall.

A striking characteristic of the intestinal innervation was that each arterial branch, beginning at the major named branches (cf. Boekellar et al. 1985) and then continuing with the secondary and tertiary branches produced by the successive bifurcations of the arterial tree, was joined not by a single bundle of axons, but rather by typically a pair of (and rarely three or four) distinct bundles of axons (the count of bundles was performed by microscopic inspection; 50×). This pattern can be seen in the specimens in Figs. 2b, 3a. As the vessels forked into higher-order radicles, the associated bundles containing vagal afferent fibers also divided and distributed (typically) the pair of daughter roots onto each of the more distal arterial vessels. As the pairs of bundles traveled distally toward the intestine, they often appeared to interchange small fascicles of axons (for examples of these branching patterns, see Fig. 3a,b). The pattern of paired vagal fascicles associated with each radicle consistently occurred following unilateral nodose ganglion injections (or, similarly, after unilateral injections into the nucleus of the solitary tract together with

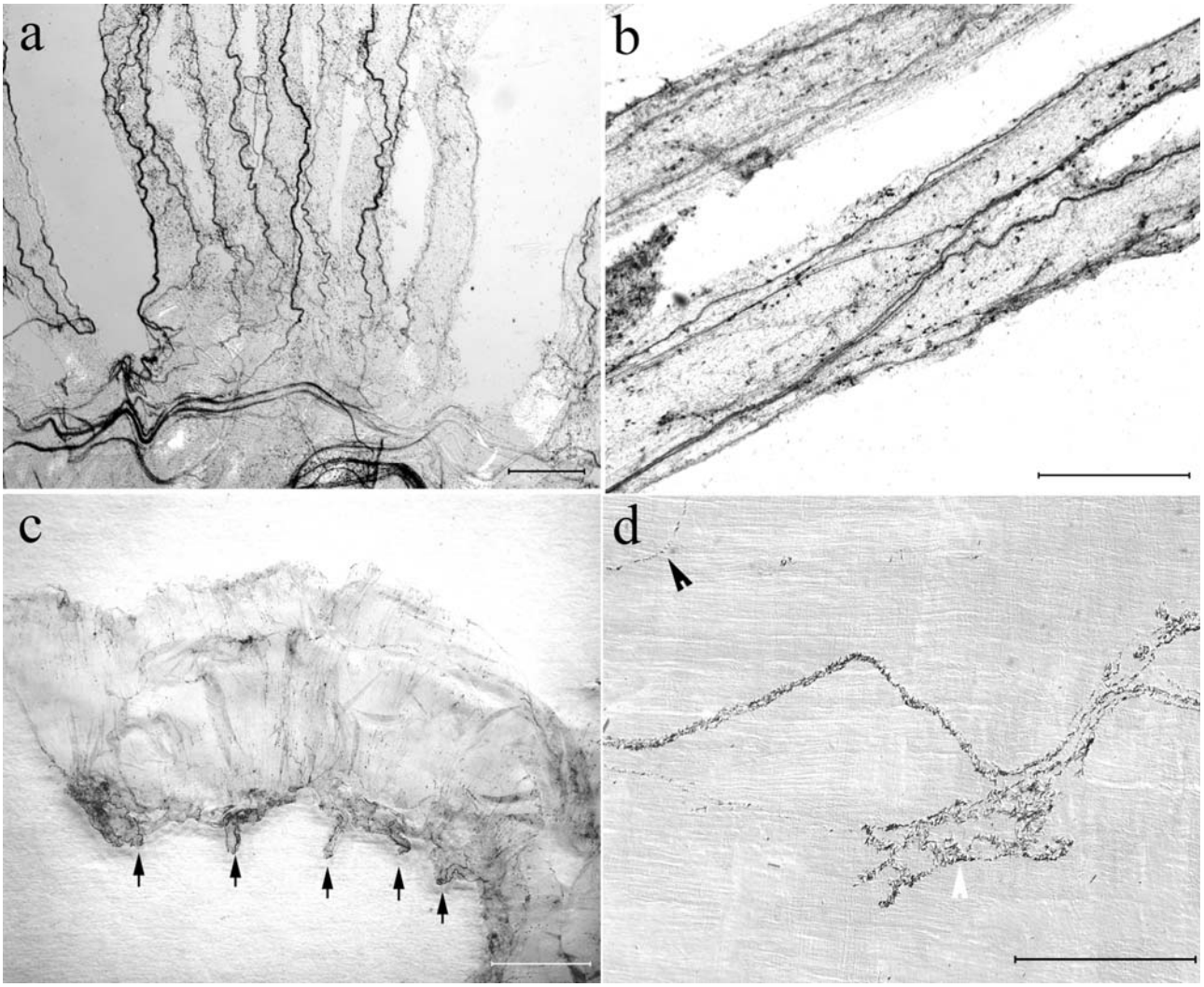

Fig. 3 Mesenteric trajectories of the vagal afferent fibers innervating the intestines. **a** Fascicles of vagal afferents originating from the celiac branches of the vagus (labeled by bilateral injections in the nucleus of the solitary tract) can be seen coursing on the wall of the SMA (*bottom*). Paired bundles of afferents can also be observed coursing vertically on several of the jejunal arterial branches arising from the SMA. **b** Vagal afferent bundles can be observed on arterial branches traveling toward the intestines. In this view, two arterial branches run from *lower left* toward the intestines (*above* and to the *right*). The *lower* of the two arteries branches in the field of view, and the bundles of afferents can be observed bifurcating and re-sorting to maintain multiple bundles on each of the daughter branches of the bifurcating artery. All bundles of afferents were labeled here by a unilateral injection of the left nodose ganglion. The *black spots* on the arterial walls are mast cells. **c** A jejunal segment processed with the *en bloc* WGA-HRP protocol. Vagal afferents were labeled via an injection into the right nodose ganglion (*arrows* stubs of neurovascular bundles divided by dissection just superficial to the wall of the intestine. The small *black dots* in the wall of the intestine are individual afferent endings, viz., intraganglionic laminar endings (see **d**). **d** TMB labeling of an individual afferent terminal, viz., an intraganglionic laminar ending (*white arrowhead*) in the wall of the colon at higher magnification. A bundle of a few vagal afferent fibers courses horizontally just *above* the intraganglionic laminar ending (*black arrowhead* single labeled afferent fiber). Tissue specimen from an animal that had received a unilateral injection of WGA-HRP into the left nodose ganglion. *Bars* 300 μm (**a**, **b**), 5 mm (**c**), 150 μm (**d**)

contralateral cervical vagotomies). Hence, vagal afferents must re-sort peripherally so that both left and right nodose ganglion fibers are found in both fascicles of a pair.

The segment of jejunum in Fig. 3c illustrates the pattern of vagal afferent innervation as each of the terminal arterial branches reaches the intestinal surface. Stubs of neurovascular radicles can be seen where they were sectioned and separated from the arterial tree. At this level, the fine jejunal arteries enter the organ at approximately every 5 mm, and each of the arteries carries two fascicles of vagal afferents. Once the nerve bundles reach the wall of the intestine, they ramify into individual axons or fascicles of a few axons and run, predominately in a circular direction and secondarily or more limitedly with a longitudinal orientation, over limited distances before ending in terminal fields. In another illustration of the capability of the *en bloc*

WGA-HRP method to penetrate specimens, the extremely fine black elements that are barely visible at low power (Fig. 3c) can be seen, at higher magnification, to be terminal processes, such as individual intraganglionic laminar endings associated with myenteric ganglia in the intestinal wall (see Fig. 3d for an ending in the wall of the transverse colon).

Given that the vagal celiac branches fasciculate extensively on the abdominal aorta and produce a complex network of small bundles of axons (see Fig. 2b; also bottom of Fig. 3a) that appear to course selectively onto the SMA, we also evaluated whether any of the small bundles originating from the celiac branches continued distally on the descending aorta to course with the inferior mesenteric artery (IMA). In the sample of 15 specimens in which the descending aorta and IMA were preserved, processed, and examined, no labeled vagal axons were found running with the IMA.

Discussion

This study had two objectives. The first was to develop and evaluate an *en bloc* WGA-HRP processing procedure that would delineate the pathways or trajectories of fine peripheral nerves that, when unstained, could not be readily dissected with any certainty with regard to identity. The second goal was to apply the *en bloc* protocol to the vagal innervation of the intestines in order to improve our understanding of the course of these projections between their separation from the abdominal vagal trunks and their entry into the intestinal wall. The results will be considered in terms of these two general objectives.

Strengths and limitations of the *en bloc* HRP protocol

From a technical perspective, the *en bloc* HRP protocol has been established as practical and versatile. Use of TMB processing makes it practical to stain vagal afferent fibers labeled with WGA-HRP in the nerve trunk, within successively higher order branches of the nerves, even in fascicles that appear to be comprised of only a few axons (e.g., Fig. 3b,d) and in the walls of the target organs (e.g., Figs. 1, 3d). With appropriate processing times, TMB and the other reagents employed in routine HRP processing are readily able (unlike many techniques that rely on antibodies or larger molecules) to penetrate epineurium, serosa, and smooth muscle to stain effectively the labeled vagal axons. In additional observations (unpublished), we have observed that vagal afferents can also be effectively stained *en bloc* in the body of the esophagus (intraganglionic laminar endings; Berthoud et al. 1997) and that vagal and glossopharyngeal afferents can similarly be stained in the thoracic arteries and aortic arch (putative baroreceptor terminals). We have not attempted to determine systematically the maximum depth of penetration that can be achieved in the various organs. However, since the reagents are aqueous solutions, adipose tissue tends to block penetration.

In terms of technique, one feature turned out to be particularly useful: incubations of the tissue could be run under direct visual control. After an initial series of animals had been processed with a sufficient range of reagent concentrations and incubation times to give confidence that staining was complete and to delineate the basic patterns of the projections, we were able to optimize processing for a particular feature through visual inspection (like traditional tray processing of a photographic print). For inspection of the finer details or the elements deep in the organ wall, the incubations could be run longer, whereas for illustrations of the paths of the major bundles (with less background artifact), processing could be shortened (e.g., the vagus in the myenteric plexus could be strongly stained, as in Fig. 1a, or could be left lightly or nearly unstained, as in Fig. 1b,c). Processing of a particular feature could also be optimized by dissection or by blocking or pinning out of the specimen, so as to enhance either visibility or penetration. Since endogenous peroxidases compete with HRP for the chromagen substrate, processing with inspection also makes it practical to optimize the staining of the labeled neurites in tissues varying in endogenous enzyme activity.

A comparison of the present *en bloc* WGA-HRP protocol with one of the few alternative techniques that has provided similarly detailed information about the microanatomy of the autonomic nervous system (ANS), namely acetylcholinesterase (AChE) staining, highlights both the limitations and strengths of the present technique. Baljet, Boekellar, Drukker, Groen, and colleagues have produced a series of elegant descriptions of autonomic pathways in the abdomen and elsewhere with an in toto AChE staining method (Baljet and Drukker 1979; Bloot et al. 1984; Baljet and Groen 1986) and have used the technique for fetal to adult tissue from a variety of species from rat to humans. This range of ages and species illustrates the versatility of the Baljet technique. However, the range cannot readily be duplicated with the present protocol. Our *en bloc* adaptation of the HRP technique requires injecting the tracer pre-mortem and hence can be used only with difficulty in fetuses and is not applicable for human tissue. The in toto AChE technique probably also can be executed more efficiently, routinely, and economically than the *en bloc* adaptation of the WGA-HRP protocol.

Additional limitations of the *en bloc* method are basically the same limitations that apply to TMB processing of HRP in general. Whereas the technique is highly

sensitive, it does not provide the high-definition labeling and staining of axons and terminals that can readily be achieved with diaminobenzidine-processing of HRP or with other tracers (see, for example, Powley and Phillips 2005). Furthermore, with the types of fixation that work best for TMB processing, the grainy crystalline reaction product tends to deteriorate in prolonged storage. We have successfully stored the material refrigerated for 6 or more months, but over time there is progressive degradation of the stain and the tissue.

The *en bloc* adaptation of the WGA-HRP does, however, offer several features that cannot be readily achieved with the AChE technique. Since WGA-HRP can be injected into a specific cell field, a specified subpopulation of autonomic efferents or afferents can easily be labeled selectively. In contrast, the in toto AChE technique labels indiscriminately both arms of the ANS, making it often impractical to decide unambiguously that a particular nerve fascicle is from a particular branch of the ANS or, even more restrictively, from a particular subpopulation of preganglionic neurons. Furthermore, the WGA-HRP adaptation can, as in the present work, be used to label visceral afferents that do not express AChE and, thus, that could not be stained with the AChE method. Moreover, the WGA-HRP technique should be readily applicable to other motor and sensory systems, in addition to those of the ANS. Finally, the ready compatibility of the WGA-HRP protocol with selective nerve cut strategies (such as the vagal efferent rhizotomy employed for the specimen in Fig. 1c) is another strength of the protocol.

Vagal afferent projection pathways to the intestines

When taken together with previous observations on the innervation of the intestines, the present results offer a relatively complete description of the vagal innervation of the small and large intestines. Vagal afferents have been previously shown to innervate the intestines, from the pylorus to the descending colon (e.g., Wang and Powley 2000). Furthermore, previous tracer experiments have shown that fine bundles of afferent vagal fibers, originating from the gastric and hepatic branches of the vagus, course superficially in the wall of the GI tract to travel from the gastric antrum across the pylorus to the intial segment, or bulb, of the duodenum. Moreover, as is illustrated in Fig. 1b,c, a descending branch(es) separating from the common hepatic branch also reaches the proximal duodenum. Both in its terminal field and in its multiple pathways through the different primary branches of the vagus nerve, this most proximal component of the vagal afferent innervation of the small intestine seems to parallel the distribution of vagal efferents to the initial segment of the duodenum (cf. Berthoud et al. 1991).

In contrast to these established details, the more distal and circuitous pathways of the afferents traveling in the celiac branches of the vagus has, at best, only been sketchily understood, and the present results add a number of details to that picture. Celiac branch vagal afferents to the intestines arch up to the abdominal aorta in association with the left gastric artery and its parent celiac artery. As the celiac branches course in proximity to the celiac ganglia and wrap onto the SMA, they break into a number of smaller secondary and higher order branches. On the SMA, these fascicles of the celiac afferents appear to sort, reorganize, and reassemble so that (typically) pairs of fascicles separate to travel with each of the arteries derived from the SMA to the intestines. As the major arteries given off by the SMA bifurcate into successively finer higher order vessels, the pairs of vagal fascicles also divide in a pattern that includes axons from each of the parent pair of fascicles in each of the higher order pair of fascicles that continue to the intestines with each of higher order arterial branches. Of note, although the afferent projections to the pancreas are not the focus of the present work, this same type of projection pattern seems to occur for the small pancreatic arteries that originate from the SMA.

Without a protocol such as the present *en bloc* HRP method, observations of the particular trajectories of vagal afferents to the intestines are not practical. Neither dissection techniques nor non-specific staining strategies are capable of describing this detailed organization. However, in a general way, the pattern of organization described here has been anticipated by, and thus corroborated by, earlier physiological and electrophysiological observations (e.g., Downman 1952; Morrison 1977). Although these physiological approaches are nicely complementary to the present tracer analysis, the full complexity of the pathways (e.g., multiple re-sortings and re-aggregations of fascicles, exhaustive sorting onto each artery, sets of fascicles associated with even higher order arteries) can be more simply and definitively established by a morphological strategy such as the present *en bloc* HRP adaptation.

The organization of vagal afferents observed in the present study also corroborates and elaborates two recent reports of the distribution of vagal afferent terminals in the intestines (i.e., Phillips et al. 1997; Wang and Powley 2000). First, traditionally, the vagal innervation of the more distal intestines has been assumed to be sparse or possibly even non-existent. In contrast, however, using a WGA-HRP mapping strategy to produce an inventory of vagal afferent terminals in the GI tract, we have found that the vagus provides afferents to the distal bowel, even to the level of the mid- or transverse colon (Wang and Powley 2000; for similar efferent pattern, see Altschuler et al. 1991, 1993). The present observations that conspicuous fascicles of

vagal afferents course with the middle colic (supplying the transverse colon), right colic (supplying the ascending colon), and the ileocecocolic (supplying the ileum, cecum, and proximal colon) arteries substantiate the same point and also indicate the pathways by which vagal afferents reach the various intestinal regions. Second, the hepatic branch of the vagus, presumably because of its name and conspicuous secondary bundle turning onto the portal vein and coursing toward the liver hilus, has traditionally been considered in terms of its hepatic projections. As previously reported (Phillips et al. 1997), however, the hepatic branch of the vagus also supplies afferents not only to the stomach and proximal duodenum, but also to the ileum and ileocecal junction. Although labeling has not been combined with selective abdominal branch cuts in the present study, the vagal afferent fascicles that we have observed distributing along the SMA and its derivative arteries probably consist not only of celiac branch fibers, but also of hepatic (and conceivably gastric) branch afferents.

Acknowledgements We thank Dr. Robert Phillips for his expert help in the production of the figures.

References

Altschuler SM, Ferenci DA, Lynn RB, Miselis RR (1991) Representation of the cecum in the lateral dorsal motor nucleus of the vagus nerve and commissural subnucleus of the nucleus-tractus-solitarii in rat. J Comp Neurol 304:261–274

Altschuler SM, Escardo J, Lynn RB, Miselis RR (1993) The central organization of the vagus nerve innervating the colon of the rat. Gastroenterology 104:502–509

Baljet B, Drukker J (1979) Extrinsic innervation of the abdominal organs in the female rat. Acta Anat 104:243–267

Baljet B, Groen GJ (1986) Some aspects of the peripheral nervous-system in the human-fetus as revealed by the acetylcholinesterase in toto staining method. Acta Histochem Suppl 32:69–75

Berthoud HR, Powley TL (1992) Vagal afferent innervation of the rat fundic stomach: morphological characterization of the gastric tension receptor. J Comp Neurol 319:261–276

Berthoud H-R, Carlson NR, Powley TL (1991) Topography of efferent vagal innervation of the rat gastrointestinal tract. Am J Physiol 260:R200–R207

Berthoud HR, Kressel M, Raybould HE, Neuhuber WL (1995) Vagal sensors in the rat duodenal mucosa—distribution and structure as revealed by in-vivo DiI-tracing. Anat Embryol 191:203–212

Berthoud HR, Patterson LM, Neumann F, Neuhuber WL (1997) Distribution and structure of vagal afferent intraganglionic laminar endings (IGLEs) in the rat gastrointestinal tract. Anat Embryol 195:183–191

Bloot J, Boekellar AB, Baljet B (1984) A simple acetylcholinesterase method for staining in toto the nervous-system in rat fetuses and a procedure for embedding stained fetuses in transparent epoxy-resin. Stain Tech 59:246–249

Boekellar AB, Baljet B, Drukker J (1985) The arterial vascular supply of the upper abdominal organs in the rat. Neth J Zool 35:455–468

Boekellar AB, Groen GJ, Baljet B (1987) Anatomy of the abdominal branches of the vagus nerves in the rat. Acta Anat 130:12–13

Downman CBB (1952) Distribution along the small intestine of afferent, vasoconstrictor and inhibitory fibres in the mesenteric bundles. J Physiol (Lond) 116:228–235

Fox EA, Powley TL (1985) Longitudinal columnar organization within the dorsal motor nucleus represents separate branches of the abdominal vagus. Brain Res 341:269–282

Hebel R, Stromberg MW (1976) Anatomy of the laboratory rat. Williams & Wilkins, Baltimore, pp 91–111

Holst M-C, Kelly JB, Powley TL (1997) Vagal preganglionic projections to the enteric nervous system characterized with PHA-L. J Comp Neurol 381:81–100

Hopkins DA, Bieger D, deVente J, Steinbuisch HWM (1996) Vagal efferent projections: viscerotopy, neurochemistry and effects of vagotomy. Prog Brain Res 107:79–96

Mesulam M-M (1978) Tetramethyl benzidine for horseradish peroxidase neurohistochemistry: a non-carcinogenic blue reaction-product with superior sensitivity for visualizing neural afferents and efferents. J Histochem Cytochem 26:106–117

Mesulam M-M (1982) Principles of horseradish peroxidase neurohistochemistry and their applications for tracing neural pathways—axonal transport, enzyme histochemistry and light microscopic analysis. In: Mesulam M-M (ed) Tracing neural connections with horseradish peroxidase. Wiley, Chichester, pp 1–151

Morrison JFB (1977) The afferent innervation of the gastrointestinal tract. In: Brooks FP, Evers PW (eds) Nerves and the gut. Slack, New Jersey, pp 297–326

Phillips RJ, Baronowsky EA, Powley TL (1997) Afferent innervation of gastrointestinal tract smooth muscle by the hepatic branch of the vagus. J Comp Neurol 384:248–270

Powley TL, Phillips RJ (2005) Advances in neural tracing of vagal afferent nerves and terminals. In: Undem BJ, Weinreich D (eds) Advances in vagal afferent neurobiology. CRC Press, Boca Raton, pp 123–145

Powley TL, Prechtl JC, Fox EA, Berthoud H-R (1983) Anatomical considerations for surgery of the rat abdominal vagus: distribution, paraganglia and regeneration. J Auton Nerv Syst 9:79–97

Powley TL, Fox EA, Berthoud H-R (1987) Retrograde tracer technique for assessment of selective and total subdiaphragmatic vagotomies. Am J Physiol 253:R361–R370

Prechtl JC, Powley TL (1985) Organization and distribution of the rat subdiaphragmatic vagus and associated paraganglia. J Comp Neurol 235:182–195

Prechtl JC, Powley TL (1987) A light and electron microscopic examination of the vagal hepatic branch of the rat. Anat Embryol 176:115–126

Prechtl JC, Powley TL (1990) The fiber composition of the abdominal vagus of the rat. Anat Embryol 181:101–115

Robertson B, Lindh B, Aldskogius H (1992) WGA-HRP and choleragenoid-HRP as anterogradely transported tracers in vagal visceral afferents and binding of WGA and choleragenoid to nodose ganglion neurons in rodents. Brain Res 590:207–212

Walls EK, Wang FB, Holst M-C, Phillips R, Voreis JS, Perkins AR, Pollard LE, Powley TL (1995) Selective vagal rhizotomies: a new dorsal surgical approach used for intestinal deafferentations. Am J Physiol 269:R1279–R1288

Wang FB, Powley TL (2000) Topographic inventories of vagal afferents in gastrointestinal muscle. J Comp Neurol 421:302–324

Zhang XG, Fogel R, Simpson P, Renehan W (1991) The target specificity of the extrinsic innervation of the rat small-intestine. J Auton Nerv Syst 32:53–62

Zhang XG, Renehan WE, Fogel R (2000) Vagal innervation of the rat duodenum. J Auton Nerv Syst 79:8–18